

DEVELOPING TSUNAMI FRAGILITY FUNCTIONS USING NUMERICAL MODELING AND REMOTE SENSING DATA FROM THE 2010 CHILE TSUNAMI

Geronimo Pulido I.¹
MEE20714

Supervisor: Shunichi KOSHIMURA²
Yushiro FUJII^{3*}, Bunichiro SHIBAZAKI^{3**},
Toshiaki YOKOI^{3**}, Masaru SUGAHARA^{4**}

ABSTRACT

On February 27, 2010, a megathrust earthquake of Mw 8.8 (USGS) provoked a destructive tsunami in Chile. The tsunami damaged about 600 km area along the coast of Chile, including the coastal towns of Dichato and Tumbes in the Bio-Bio region and Robinson Crusoe Island on the archipelago of Juan Fernandez, about 670 km off the coast of Chile. To estimate the structural damage in a quantitative manner for the areas mentioned, tsunami fragility functions were developed. Using Tohoku University's Numerical Analysis Model for Investigation of Near-field tsunamis (TUNAMI) for the numerical simulation to obtain the propagation and inundation depths and visual inspection of satellite images for the damage data, the fragility curves for Juan Fernandez, Tumbes, and Dichato were constructed. The obtained curves suggest that for an inundation depth of one meter, the damage probability is 7%, 48%, and 82% for Tumbes, Dichato, and Juan Fernandez, respectively. The similarity of the construction type (wood, masonry, and mixed) indicates that the areas' exposure and building configuration has the most significant impact on the structural damage, considering that Juan Fernandez island was not affected by the ground motion of the 2010 event.

Keywords: Tsunami, Fragility function, 2010 Maule Earthquake, Chile.

1. INTRODUCTION

Chile is a country that is constantly affected by catastrophic events such as earthquakes and tsunamis. On February 27, 2010, local time 3:34:08 AM, an earthquake of Mw 8.8 (USGS) attacked the Maule region, becoming the second-largest event in the country's history following the great earthquake of Valdivia in 1960, the largest event in our country's history. The 2010 earthquake affected most of the country's central zone, where an estimated 13 million people lived at that time. After this event, many vulnerabilities were exposed, and the need for new and better mitigation measures against tsunamis became evident. To assess the structural damage, fatality, or vulnerability due to a tsunami attack, Koshimura et al. (2009) proposed tsunami fragility functions as a tool to quantify the damage probability by constructing them from the integration of satellite remote sensing, field surveys, and numerical modeling with geographic information system (GIS). In this work, fragility curves are developed for the three cities, Dichato, Tumbes, and Juan Fernández, affected by the 2010 tsunami using remote sensing and satellite images for the damage interpretation and numerical modeling to obtain the hydrodynamic features of the tsunami.

¹ Chilean Association of Port and Coastal Engineering (ACHIPYC), Chile.

² Professor, International Research Institute of Disaster Science (IRIDeS), Tohoku Univ.

³ International Institute of Seismology and Earthquake Engineering (IISEE), Building Research Institute (BRI).

⁴ National Graduate Institute for Policy Studies (GRIPS).

* Chief examiner, ** Examiner

2. DATA

2.1. Bathymetry and topography data

For the present work, four-nested grid systems (Figures 1 and 2) were generated for the numerical modeling using GEBCO's 2021 15 arc-second gridded bathymetric data (GEBCO Compilation Group, 2021), bathymetric probes data associated with the Hydrographic and Oceanographic Service of the Navy (SHOA) nautical charts No. 5411, 6000, 6110, and 6120, and LIDAR bathymetric surveys data provided by Rafael Aránguiz Associate Professor of Universidad Católica de la Sma Concepción (Bio-Bio region). To characterize the inundation, we used the land elevation one arc-second grid mesh data from the Shuttle Radar Topography Mission (SRTM), a topographic survey conducted by the Ministry of National Property of Chile, and LIDAR topographic surveys merged with the bathymetry data for the highest resolution grids.

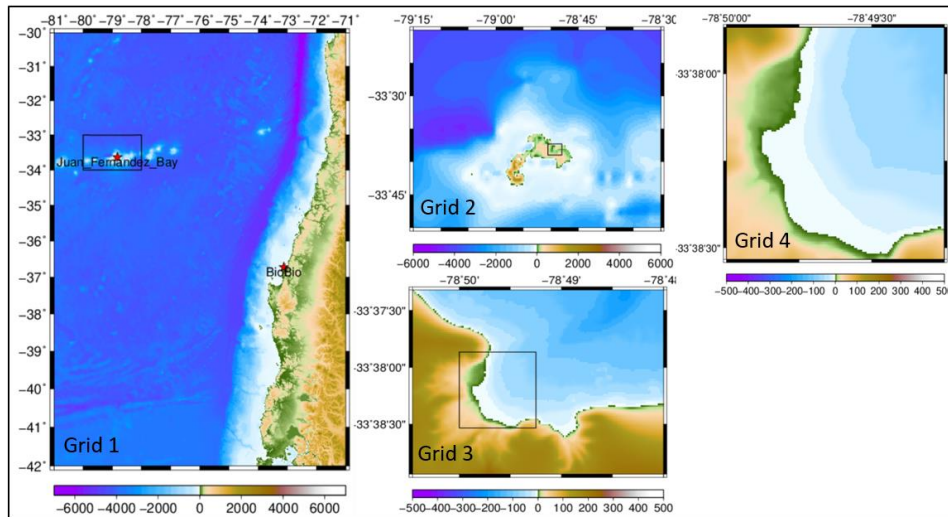


Figure 1. Model setting of nested computational grids for Juan Fernández.

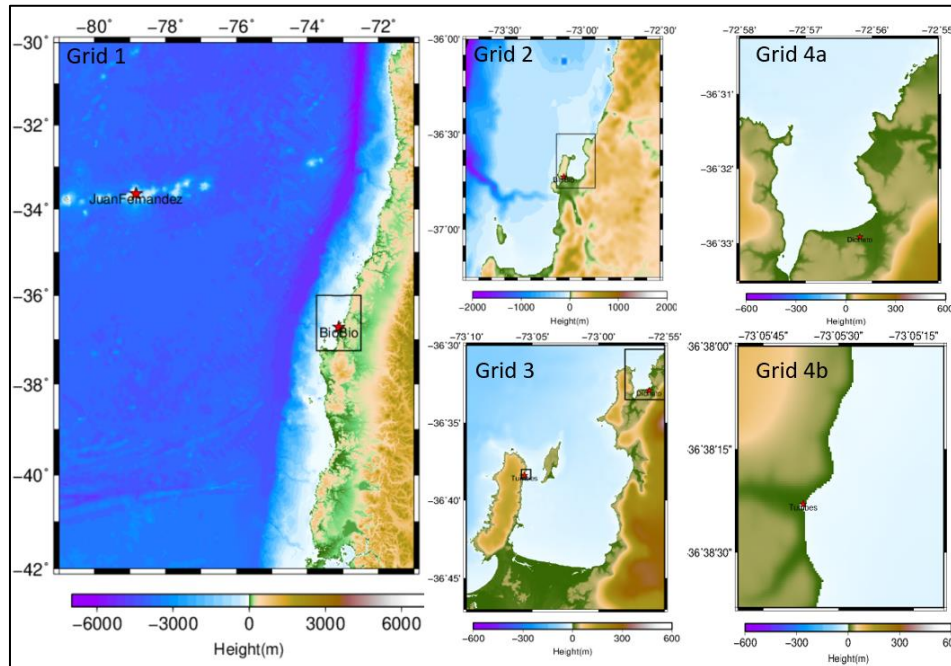


Figure 2. Model setting of nested computational grids for Bio-Bio region. The finest grids 4a and 4b correspond to Dichato and Tumbes, respectively.

2.2. Damage data collection

The Chilean Air Force (SAF) has sets of aerial photographs before and after the day of the tsunami impact at a scale of 1:10,000. The identification of the destroyed houses for Juan Fernández Island was made by comparing frame No. 55409 dated 21-01-2009 with frames No. 324454 to 324457 dated 28-02-2010. For the Bio-Bio region, high-resolution satellite images dated 03-06-2010 were obtained from the web site (<http://www.digitalglobe.com>) and compared with Google Earth satellite images of 09-10-2009.

3. METHODOLOGY

3.1. Building structure damage data set

The interpretation and classification of the structures affected by the tsunami were carried out visually by inspecting high-resolution satellite images before and after the tsunami. The high resolution of the images is critical to distinguish the degree of damage of the structure only through the state of the roofs. This method has the advantage of allowing us to visually understand structural damage and its extent on a regional scale. To obtain a damage statistic set, the structures are spatially sampled in the calculated inundation zone and sorted by inundation ranges. With the number of structures for each inundation range and the number of wash-away/destroyed buildings, we can determine the damage probability associated with each inundation group.

3.2. Tsunami simulation

In this study, the numerical modeling was carried out using the TUNAMI code, the version compiled by Yanagisawa (2021). This software is a tsunami numerical simulation program that uses the linear wave theory for deep-sea and the shallow wave theory for simulation near the coast. The program runs with bathymetry/topography data and fault parameters as input, and outputs several sea states at different times and locations.

The slip distribution inverted from DART, tide gauge, GPS, and coastal geodetic data by Yoshimoto et al. (2016) was used. In this model, 44 subfaults (11 x 4) were assumed with the subfault areas of 50 km x 50 km and 50 km x 25 km for the shallowest ones, the rake and strike angles were set to 16° and 105°, respectively, the depth-dependent dip angles of 10°, 18° and 24° were set from the trench towards down-dip, and the depths of the subfaults ranged from 0 to 28.4 km in the down-dip direction.

3.3. Tsunami fragility

It is defined as the structural damage probability related to the hydrodynamic features of the tsunami flow. Developing the fragility functions, we used the same approach that researchers in the tsunami risk assessment field took from the earthquake engineering studies of risk analysis to construct the tsunami fragility curves. In those studies, the fragility functions are defined by the following Eq. (1) or Eq. (2);

$$P_D(x) = \Phi \left[\frac{\ln x - \lambda}{\xi} \right] = \int_{-\infty}^x \frac{1}{\sqrt{2\pi}\xi t} \exp \left(-\frac{(\ln t - \lambda)^2}{2\xi^2} \right) dt \quad (1)$$

$$P_D(x) = \Phi \left[\frac{x - \mu}{\sigma} \right] = \int_{-\infty}^x \frac{1}{\sqrt{2\pi}\sigma} \exp \left(-\frac{(t - \mu)^2}{2\sigma^2} \right) dt \quad (2)$$

, where $P_D(x)$ is the damage probability, Φ the standardized lognormal or normal cumulative distribution function, λ (or μ) is the mean of $\ln x$ (or x), and ξ (or σ) is the standard deviation of $\ln x$ (or x).

Once we compile the set of damage probability data related to its hydrodynamic feature obtained from the inundation model, we plot them versus $\ln x$ or x from Eq. (1) or (2) and invert the ϕ function by applying the least-square fitting to the plot. We can obtain the mean and the standard deviation from these plots and finally construct the fragility function.

4. RESULTS AND DISCUSSION

The slip distribution by Yoshimoto et al. (2016), which was obtained using only the tsunami waveform records at 26 DARTs reproduces a better agreement with inundation areas and depths at the study sites (Figure 3). The tsunami travel times in the model are similar to those reported on February 27 (Fritz et al., 2011), reaching to the Juan Fernández bay in approximately 49 minutes.

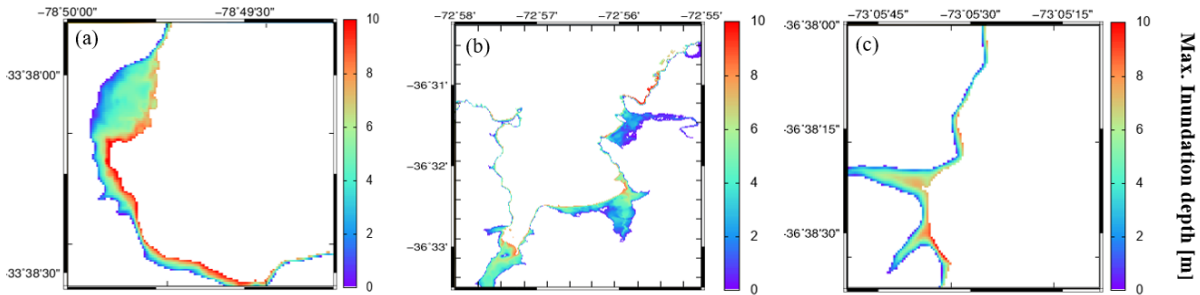


Figure 3. Tsunami maximum inundation depths obtained from the source model (Yoshimoto et al., 2016) inverted from DART data at (a) Juan Fernandez, (b) Dichato, and (c) Tumbes.

Once the tsunami hazard estimation was obtained, we spatially related the damage data determined by comparing the before and after images of the study sites and compiled the damage probability data related to its hydrodynamic feature, inundation depth in this study (Figure 4).

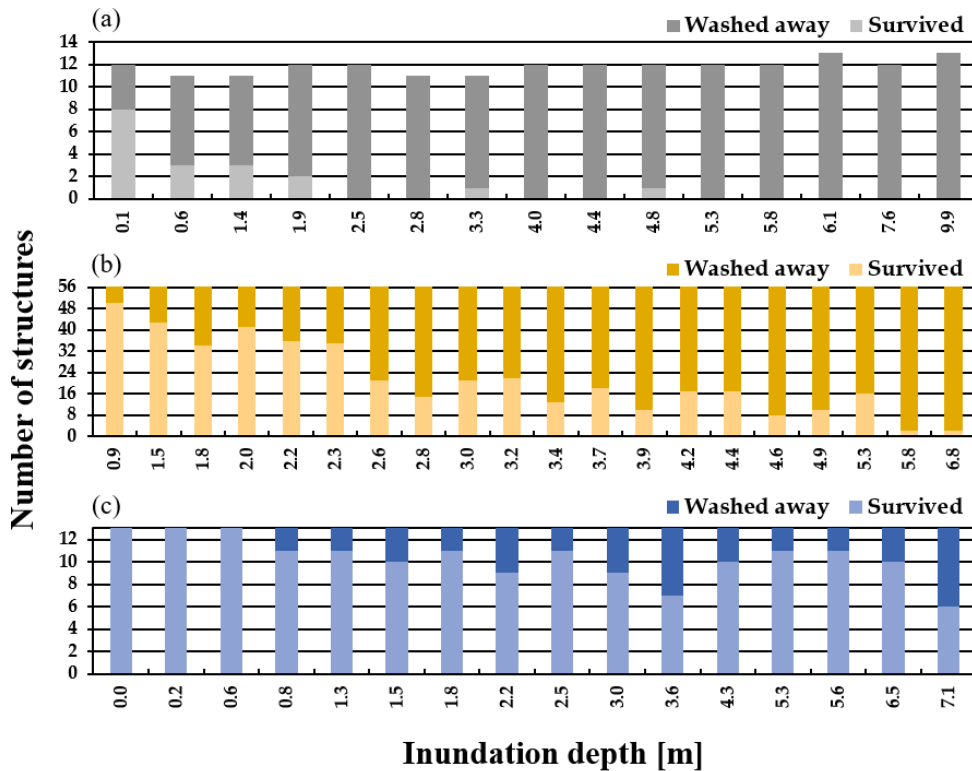


Figure 4. Histograms of the numbers of washed-away and survived structures in terms of inundation depth ranges within the tsunami inundation zones at (a) Juan Fernández, (b) Dichato, and (c) Tumbes.

Following the steps mentioned in the section 3, the damage probabilities were obtained for the median values of inundation depths. Through a linear regression analysis, the relation between these damage probabilities and the inundation depths were explored. Plotting $\ln x$ from Eq. (1) and the $\phi-1$ function, we obtained the statistical parameters (Table 1) to construct the fragility functions.

Table 1. Statistical parameters of tsunami fragility curves.

Site	Standard deviation ξ	Mean λ
Juan Fernández	0.4938	-0.3399
Dichato	0.2738	0.3862
Tumbes	0.8445	1.0586

Eq. (1) and Eq. (2) are expressed in terms of the standard lognormal or normal cumulative distribution functions, respectively. The selection of which distribution to apply depends on the best fitting of the constructed curve and the data set. The fragility functions for Juan Fernández and Dichato were created using the lognormal distribution and the normal cumulative function for Tumbes, which shows a better agreement with the data obtained. The fragility functions obtained for the different areas with the respective damage probability distributions are shown in Figure 5.

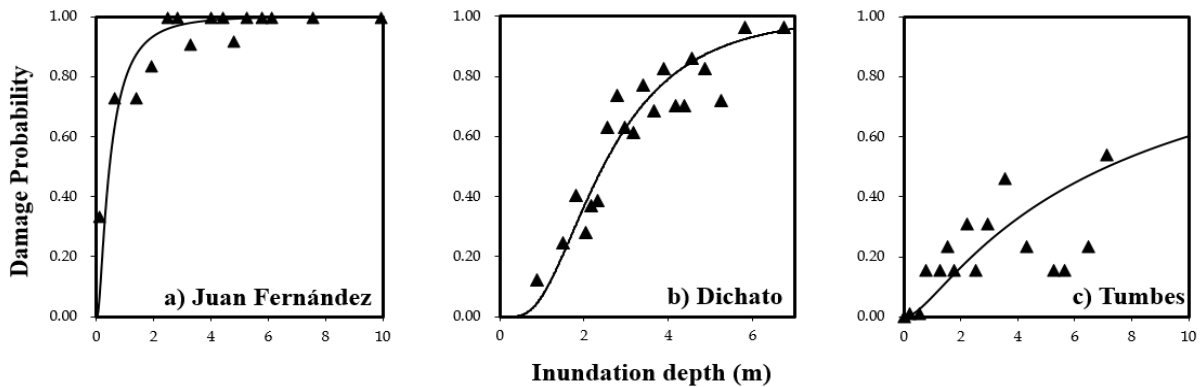


Figure 5. Fragility functions for structural damage in terms of the inundation depth at (a) Juan Fernandez, (b) Dichato, and (c) Tumbes.

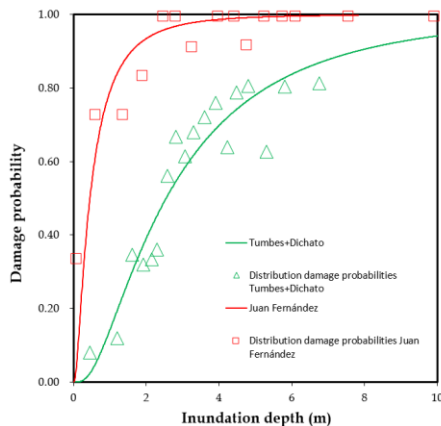


Figure 6. Fragility functions at Juan Fernández (red symbols and line) and Tumbes + Dichato (green ones).

Figure 6 compares the fragility functions obtained by combining the Tumbes and Dichato's data against the one from Juan Fernández. Since Juan Fernández Island is located at 670 km apart from the coast of Chile, the island was not suffered from the effects of the strong ground motion, and the observed structural damage is only due to the action of the tsunami. As the study sites consist of a similar construction type (wood, masonry, and the mixed type), the factors that possibly contributed to the more significant destruction in Juan Fernández can be related to the inundation flow velocity, which is directly influenced by the building distribution. In Juan Fernández, the town center is located within 200 meters from the coastline, where the horizontal inundation distance was up to 300 meters in some places, and the building density is very low compared with the other study sites. Consequently, the tsunami flow reaches greater velocities because it does not have obstacles that slow down the flow and therefore causes more significant damage to the structures. The differences

between the two fragility functions can be clearly seen. For example, damage probabilities at two meters of inundation depth are 39% and 94% for the combined sites (Tumbes and Dichato) and Juan Fernández alone, respectively.

5. CONCLUSIONS

Tsunami fragility functions were developed to quantify the damage probability of structures within an exposed area from a tsunami attack. Using numerical tsunami modeling and high-resolution satellite images of before and after the event, the tsunami fragility functions for the 2010 Maule earthquake and tsunami in terms of the inundation depth were constructed for Dichato and Tumbes in the Bio-Bio region and Juan Fernandez Island. Two levels ("survived" and "destroyed") for classification of structural damage were used. The numerical modeling results spatially referenced were compared with field survey measurements to obtain some grade of validation of the calculations. In the case of Tumbes and Juan Fernandez, the field survey measurement data were few, so the overall correlation may not be reliable even if most of the survey points show less than one meter of difference from the calculations. At Dichato, on the other hand, the numerical modeling presents a correlation of about 60% with the field survey measurements. This difference may be explained by the resolution of the topography and bathymetry data, the approximation of building structure type, and the overall exposure of the city.

A comparison between the tsunami fragility functions of earthquake-affected (Tumbes and Dichato) and non-earthquake-affected areas (Juan Fernandez) was proposed to identify possible influence factors in the damage probability. The latter shows the higher damage probability for the lower inundation depths, i.e., 79% of damage probability for one meter of inundation depth, pointing that even if the strong motion previously degraded the buildings of the areas affected by earthquakes, local effects like building distribution and exposure have significant impacts to the tsunami damage probability estimation. Many other factors not mentioned in this study may dramatically impact the analysis of the damage probability, so the tsunami fragility functions should be taken as one piece of a toolkit for a comprehensive tsunami hazard estimation.

ACKNOWLEDGEMENTS

The author would like to thank the supervisors of this work, Dr. Shunichi Koshimura, Professor, International Research Institute of Disaster Science (IRIDeS) of Tohoku University; Dr. Erick Mas, Associate Professor, IRIDeS of Tohoku University; and Dr. Yushiro Fujii, senior research scientist, IISEE, BRI, for all the guidance and advice through this work.

REFERENCES

- Fritz, H.M., Petroff, C.M., Catalán, P.A. et al. (2011). Field Survey of the 27 February 2010 Chile Tsunami. *Pure Appl. Geophys.* 168, 1989–2010. <https://doi.org/10.1007/s00024-011-0283-5>.
- GEBCO Compilation Group (2021) GEBCO 2021 Grid (doi:10.5285/c6612cbe-50b3-0cff-e053-6c86abc09f8f).
- Koshimura, S., Namegaya, Y., & Yanagisawa, H. (2009). Tsunami Fragility-A New Measure to Identify Tsunami Damage.
- Yanagisawa, H. (2021). Numerical simulation of Tsunami inundation and its application [Code]. Retrieved from IISEE Lectures notes, Disaster Management Program 2020-2021.
- Yoshimoto, M., Watada, S., Fujii, Y., & Satake, K. (2016). *Geophysical Research Letters*, 43(2), 659–665. <https://doi.org/10.1002/2015GL067181>.